Catchup: a mouse model for imaging-based tracking and modulation of neutrophil granulocytes

Anja Hasenberg[1,9], Mike Hasenberg[1,9], Linda Männ[1], Franziska Neumann[1], Lars Borkenstein[1], Manuel Stecher[1], Andreas Kraus[1], Daniel R Engel[1], Anika Klingberg[1], Pegah Seddigh[1], Zeinab Abdullah[2], Sabrina Klebow[3], Swen Engelmann[4], Annegret Reinhold[4], Sven Brandau[5], Michaela Seeling[6], Ari Waisman[3], Burkhart Schraven[4,7], Joachim R Göthert[8], Falk Nimmerjahn[6] & Matthias Gunzer[1]

Neutrophil granulocyte biology is a central issue of immunological research, but the lack of animal models that allow for neutrophil-selective genetic manipulation has delayed progress. By modulating the neutrophil-specific locus Ly6G with a knock-in allele expressing Cre recombinase and the fluorescent protein tdTomato, we generated a mouse model termed Catchup that exhibits strong neutrophil specificity. Transgene activity was found only in very few eosinophils and basophils and was undetectable in bone marrow precursors, including granulomonocytic progenitors (GMPs). Cre-mediated reporter-gene activation allowed for intravital two-photon microscopy of neutrophils without adoptive transfer. Homozygous animals were Ly6G deficient but showed normal leukocyte cellularity in all measured organs. Ly6G-deficient neutrophils were functionally normal *in vitro* and in multiple models of sterile or infectious inflammation *in vivo*. However, Cre-mediated deletion of FcγRIV in neutrophils reduced the cells' recruitment to immune-complex-mediated peritonitis, suggesting a cell-intrinsic role for activating Fc receptors in neutrophil trafficking.

Neutrophil granulocytes are essential phagocytes that function in innate immunity and are central to infection control[1]. After their generation from precursors in bone marrow, they are recruited to the circulation in baseline numbers that can be quickly increased through the action of inflammatory cytokines[2]. Circulating neutrophils recognize activated endothelium in inflamed sites and use a coordinated process of endothelial rolling, firm adhesion, transmigration[3] and chemotactic interstitial migration to reach sites of inflammation[4], pathogen invasion or sterile tissue necrosis[5].

Several mechanisms of neutrophil recruitment and tissue invasion have been elucidated, but others are unresolved. For example, Fc-γ-receptor IV (FcγRIV) is highly expressed on monocytes, macrophages, mast cells and neutrophils and activates these cells upon specific binding to IgG2 immune complexes (ICs)[6]. Deletion of FcγRIV has been shown to block neutrophil recruitment into areas of sterile autoantibody-mediated inflammation, but this could have been secondary to the defective recruitment of other affected cells[7]. Additional evidence implicates FcγRIII and FcγRIV in neutrophil activation, but their individual contributions to neutrophil recruitment *in vivo* are unclear[8].

Recruitment mediated via Ly6G, a highly specific surface receptor of murine neutrophils[9], also is debated. Ly6G ligation by antibodies *in vivo* depletes neutrophils[9,10], but its functional blockade by non-depleting antibody concentrations has yielded controversial results[11]. One study demonstrated reduced recruitment of neutrophils into areas of sterile inflammation *in vivo* and decreased neutrophil migration *in vitro*[11], but in a different study Ly6G was not necessary for neutrophil recruitment into *Staphylococcus*-infected skin[12].

All these studies have suffered from the lack of tools for selectively modulating and visualizing neutrophils *in vivo* via gene targeting using Cre recombinase and the expression of fluorescent proteins. Currently no existing animal model allows for exclusive neutrophil manipulation or visualization *in vivo*. In the most widely used mouse lines, LysM-Cre[13] and Lys-EGFP[14], the manipulation or fluorescent marking of other myeloid cell lines in addition to neutrophils is a well-known problem. Use of the human MRP8 (hMRP8) promoter enables more neutrophil-specific Cre expression, but genetic manipulation still occurs outside mature neutrophils, as Cre recombination also happens in myeloid precursors with monocytic potential[15].

To overcome these limitations, we developed a mouse model that uses an allele knocked into the *Ly6g* locus to exchange

[1]Institute for Experimental Immunology and Imaging, University Hospital, University Duisburg–Essen, Essen, Germany. [2]Institute of Experimental Immunology, Friedrich-Wilhelms-Universität Bonn, Bonn, Germany. [3]Institute for Molecular Medicine, Johannes Gutenberg–University of Mainz, Mainz, Germany. [4]Institute of Molecular and Clinical Immunology, Otto von Guericke University, Magdeburg, Germany. [5]Department of Otorhinolaryngology, University Hospital, University Duisburg–Essen, Essen, Germany. [6]Department of Biology, Institute of Genetics, University of Erlangen–Nuremberg, Erlangen, Germany. [7]Department of Immune Control, Helmholtz Centre for Infection Research (HZI), Braunschweig, Germany. [8]Department of Hematology, University Hospital, West German Cancer Center (WTZ), University Duisburg–Essen, Essen, Germany. [9]These authors contributed equally to this work. Correspondence should be addressed to M.G. (Matthias.Gunzer@uni-due.de).

RECEIVED 16 NOVEMBER 2014; ACCEPTED 19 JANUARY 2015; PUBLISHED ONLINE 16 MARCH 2015; DOI:10.1038/NMETH.3322

exon 1 of *Ly6g* for a bicistronic allele expressing Cre recombinase and the fluorescent protein tdTomato[16]. This model allows for specific genetic manipulation of neutrophils *in vivo*, as well as knockout of *Ly6g*. We found that Ly6G was not necessary for neutrophil generation and migration into inflamed sites, but that FcγRIV mediated neutrophil recruitment into areas of IC deposition in a cell-intrinsic manner.

RESULTS

Catchup: a model for studying Ly6G function and neutrophils

Ly6G is selectively expressed by murine neutrophils[11,17], which suggests that the Ly6G locus might allow for more neutrophil-selective targeting than do available systems. We generated a mouse line in which the first exon of *Ly6g* is replaced by a knock-in allele encoding Cre recombinase and the fluorescent protein tdTomato[16] separated by a self-splicing T2A peptide[18] (**Fig. 1a**). We retained the first intron and other coding or regulatory elements of the locus that mediate faithful transcriptional activity of *Ly6g*. Gene-targeted animals were verified by PCR (**Supplementary Fig. 1**).

Mice were fertile and were bred normally, and they produced offspring at expected Mendelian ratios (not shown). Leukocytes from heterozygous mice coexpressed tdTomato and Ly6G. Furthermore, only Gr-1^{bright} leukocytes expressed tdTomato, verifying the specificity for neutrophils (**Fig. 1b**). tdTomato was absent in other leukocytes, with the exception of a small population of eosinophils and basophils (**Supplementary Fig. 2**). Non-neutrophil cells constituted fewer than 2% of all tdTomato$^+$ cells.

Ly6g heterozygosity induced an ~50% reduction in surface protein levels (**Fig. 1b**), suggesting biallelic gene expression. As the expression of tdTomato was highly restricted to pathogen-catching neutrophils[19], we named this mouse line Catchup.

Homozygous Catchup mice were *Ly6g* deficient both genetically and in protein expression (**Fig. 1b** and **Supplementary Fig. 1**). This induced neutrophil resistance against depletion with anti-Gr-1 *in vivo* (**Fig. 1c** and **Supplementary Fig. 3**). The percentage of neutrophils in bone marrow was slightly but insignificantly lower than that in controls (**Fig. 1c**,**d**), although absolute counts were similar in the two groups (not shown). Numbers of neutrophils and the general leukocyte cellularity in peripheral organs were normal in *Ly6g*$^{+/-}$ and *Ly6g*$^{-/-}$ animals (**Fig. 1d** and **Supplementary Table 1**), indicating that Ly6G was not necessary for the development of neutrophils and leukocytes.

In the bone marrow of Catchup mice, tdTomato expression was restricted to CD11b$^+$ cells (**Fig. 2a**). After we crossed Catchup mice with a reporter line expressing high levels of tdTomato from a Cre-activatable CAG promoter in the *ROSA26* locus[20] (these mice were termed Catchup$^{IVM\text{-}red}$, as they allowed for intravital microscopy of red-stained endogenous neutrophils), we found efficient recombination in bone marrow neutrophils, leading to gradually increasing tdTomato expression with increasing Ly6G levels (**Fig. 2a** and **Supplementary Fig. 4**). Practically all tdTomato-expressing cells were CD11b$^+$Ly6G^{bright}, which allowed us to identify these cells as neutrophils (**Supplementary Fig. 5**). Importantly, tdTomato expression was absent in CD11b$^+$Ly6G$^-$ macrophages or other Ly6G$^-$ leukocytes (**Fig. 2a** and **Supplementary Fig. 4**). In spleen and peripheral blood, Cre activity levels reached >90% in neutrophils while remaining negative in other leukocytes, demonstrating the high efficiency and specificity of the

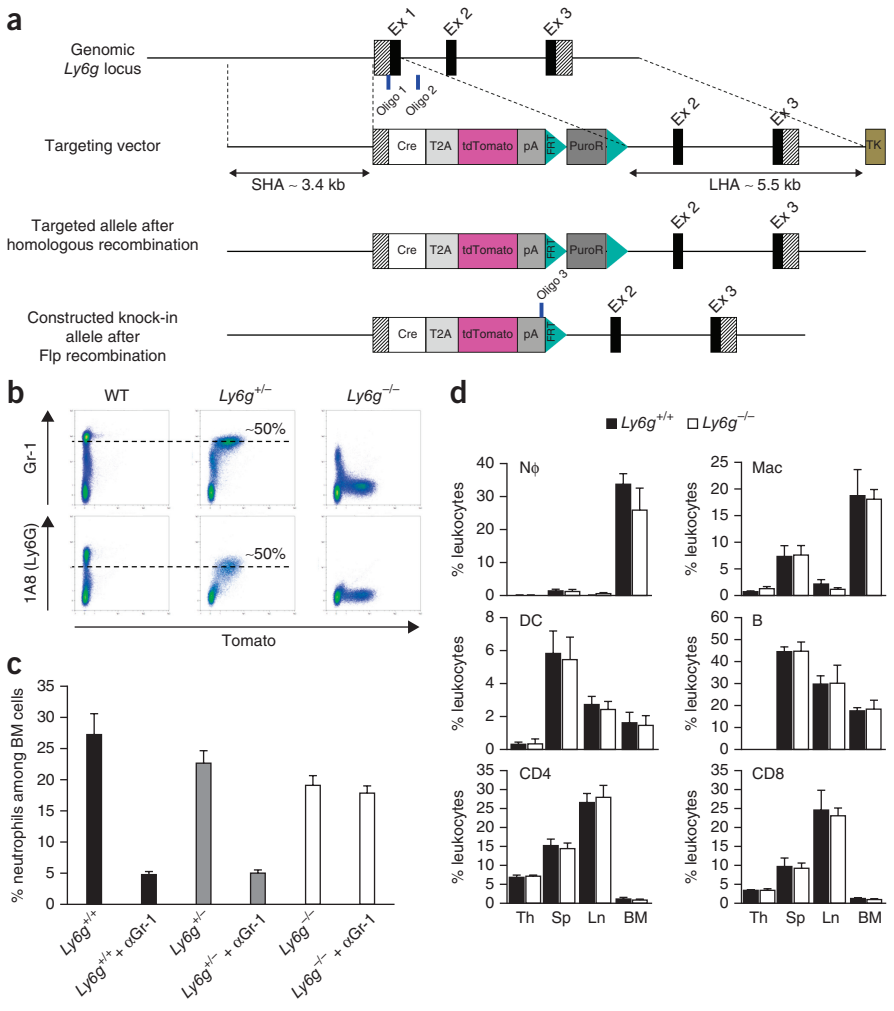

Figure 1 | Catchup, a mouse model for the genetic manipulation of neutrophils. (**a**) Targeting strategy for the generation of Catchup mice. Ex, exon. (**b**) Gr-1 and Ly6G surface expression of bone marrow cells from heterozygous and homozygous Catchup mice compared to that in wild-type (WT) animals. Representative of two independent experiments investigating a total of three animals. (**c**) Percentage of neutrophils in bone marrow (BM) with and without pretreatment with an antibody to Gr-1. Mean percentage of neutrophils + s.d. from three animals per group. (**d**) The number of leukocyte subtypes in organs of Catchup mice compared to organs of wild-type animals (Th, thymus; Sp, spleen; Ln, lymph node; Nϕ, neutrophils; Mac, macrophages; DC, dendritic cells; B, B cells; CD4, CD4$^+$ T cells; CD8, CD8$^+$ T cells). Mean percentage of cells + s.d. from four animals per group.

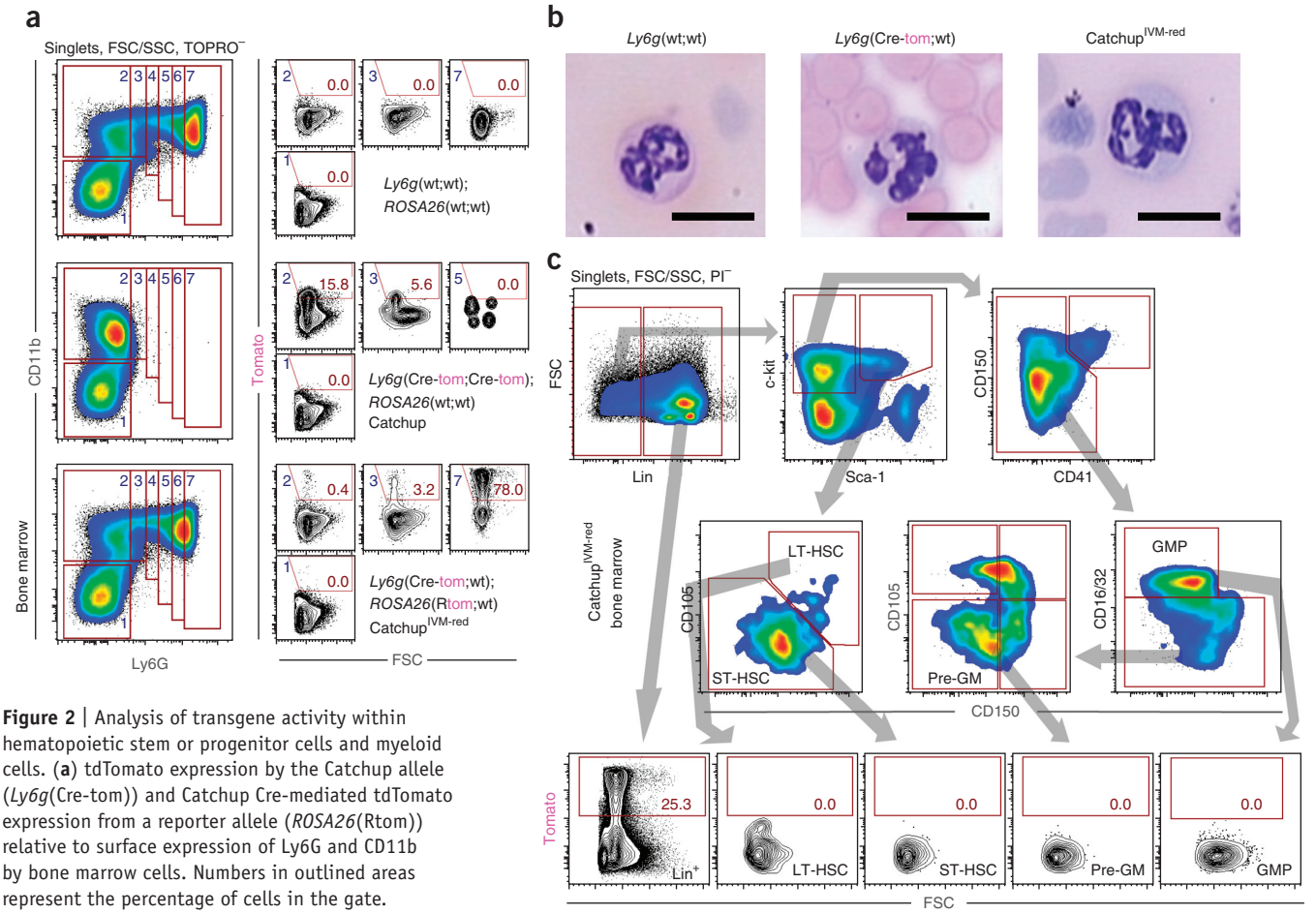

Figure 2 | Analysis of transgene activity within hematopoietic stem or progenitor cells and myeloid cells. (**a**) tdTomato expression by the Catchup allele (*Ly6g*(Cre-tom)) and Catchup Cre-mediated tdTomato expression from a reporter allele (*ROSA26*(Rtom)) relative to surface expression of Ly6G and CD11b by bone marrow cells. Numbers in outlined areas represent the percentage of cells in the gate. (**b**) Morphology of neutrophils of various genotypes. Wright–Giemsa-stained blood smears of one representative neutrophil per genotype. Scale bars, 10 µm. (**c**) Extended bone marrow flow cytometric analysis of cells from Catchup$^{IVM\text{-}red}$ mice to analyze the onset of tdTomato expression in hematopoietic precursor cells, including in GMPs. Numbers in outlined areas represent the percentage of cells in the gate. All data are representative of three analyzed animals. Lin, lineage (i.e., cells that have markers for a set of different mature leukocytes, as opposed to stem cells that do not express any of those markers); LT-HSC, long-term hematopoietic stem cell; ST-HSC, short-term hematopoietic stem cell; pre-GM, pre-granulocyte/macrophage progenitor.

transgene (**Supplementary Figs. 2** and **6**). Neutrophils from Catchup mice showed normal nuclear morphology and cytoplasmic staining in blood smears (**Fig. 2b**), and sorted tdTomato$^+$ cells from Catchup or Catchup$^{IVM\text{-}red}$ mice homogeneously appeared as neutrophils on cytospins (**Supplementary Fig. 7**). All tdTomato$^+$ leukocytes from peripheral blood of Catchup$^{IVM\text{-}red}$ mice were morphologically equal to neutrophils (forward scatter (FSC)/side scatter (SSC) values for size and granularity) and expressed high levels of CD11b and Ly6G (**Supplementary Fig. 4c**). In contrast, leukocytes expressing CD115 (macrophage colony-stimulating factor (M-CSF) receptor), and thus of the monocyte/macrophage lineage, were morphologically distinct from neutrophils and did not express Ly6G (**Supplementary Fig. 4c**) or tdTomato (**Supplementary Fig. 4d**). In the Catchup$^{IVM\text{-}red}$ mice, 90% of CD11b$^+$Ly6G$^+$ cells from peripheral blood were tdTomato^{bright}, whereas the CD115$^+$ cells were tdTomato$^-$, whether they coexpressed Ly6C or not (**Supplementary Fig. 4d**). These data showed effective and specific Cre activity within the neutrophils of Catchup mice.

A mouse line using the hMRP8 promoter for Cre expression was shown to be rather specific for neutrophils[21]. However, promoter activity in other myeloid lineages was also detectable in hMRP8 mice[22], as 10–20% of the GMP pool, which also generates macrophages[23], shows Cre activity in these mice[15]. In contrast, in Catchup$^{IVM\text{-}red}$ mice there was no Cre activity in any analyzed hematopoietic stem or progenitor population, including in GMPs, whereas transgene activity was immediately detectable upon neutrophil development (**Fig. 2c**). This explained the lack of Cre activity in peripheral leukocytes distinct from neutrophils and in a very small pool of eosinophils and basophils.

Neutrophil imaging *in vivo*

Catchup$^{IVM\text{-}red}$ mice harbored bright red neutrophils that allowed for intravital two-photon microscopy without adoptive transfer. In tibias we observed neutrophil enrichment in bone marrow at the endosteal surface (**Fig. 3a** and **Supplementary Video 1**), similar to that in cells from Lys-eGFP mice[2]. Also, motility patterns of tdTomato$^+$ cells in resting Catchup$^{IVM\text{-}red}$ mice (**Fig. 3b** and **Supplementary Video 2**) and Catchup$^{IVM\text{-}red}$ mice exposed to granulocyte colony-stimulating factor (G-CSF) (**Fig. 3c** and **Supplementary Video 3**) were similar to those previously observed[2]. *Ex vivo* microscopy in explanted bones showed stability of the red fluorescence during extended imaging sessions (**Supplementary Video 4**).

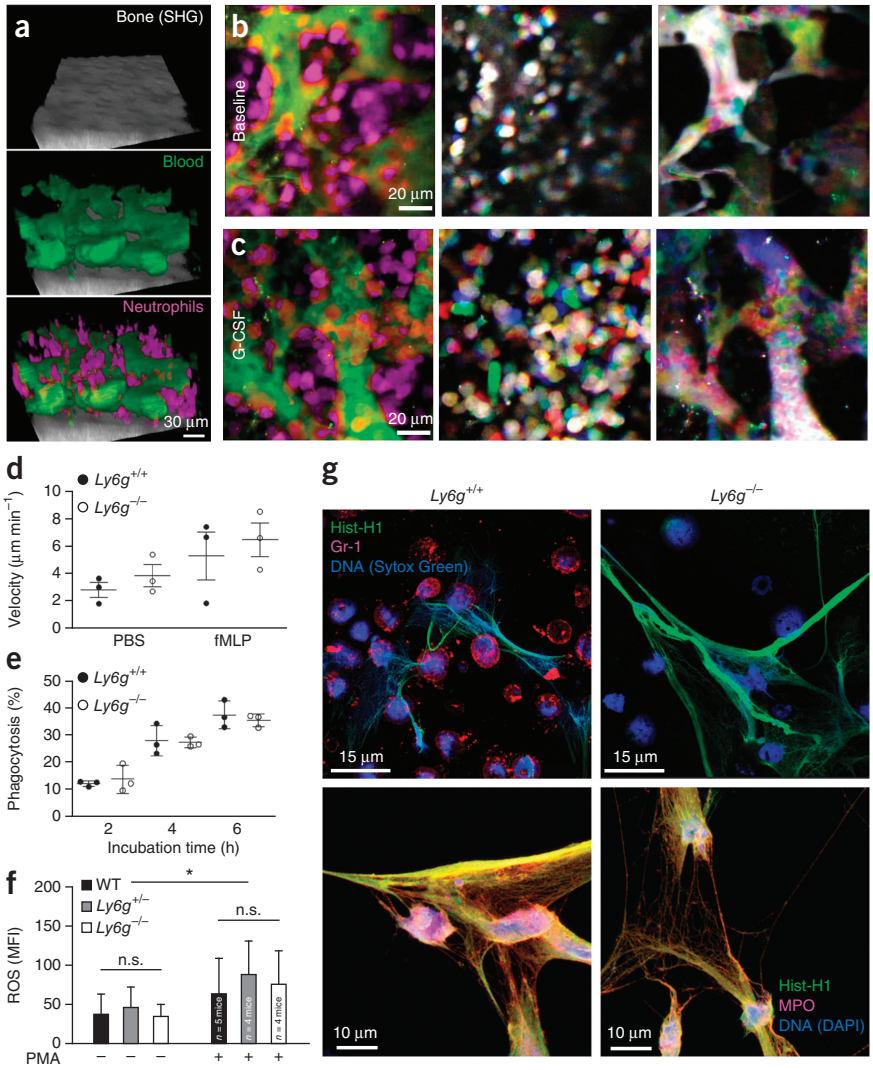

Figure 3 | Neutrophil migration *in vivo* and behavior *in vitro*. (**a**) 3D rendering of a Z-stack showing neutrophils (magenta), blood vessels (green) and bone (gray). SHG, second harmonic generation. (**b**) Motility of neutrophils (non-stimulated animal). Extended focus of neutrophils (magenta) and blood vessels (green) at one time point of a 30-min video recording (leftmost panel). Kinetic overlay (three consecutive time points) of the neutrophil (middle panel) and blood vessel channels (rightmost panel). Resting parts are white; colored parts have moved. (**c**) As in **b**, but recorded in a mouse mobilized by injection of G-CSF 2 h before imaging. (**d**) The migration of isolated neutrophils was analyzed by time-lapse video microscopy and computer-assisted cell tracking. Each circle represents the mean velocity of 15 cells measured per experiment. Lines are mean ± s.d. from three independent experiments. (**e**) Isolated neutrophils were co-incubated with *A. fumigatus* conidia and measured for internalized conidia at 2, 4 and 6 h by flow cytometry. Control animals (C57Bl/6 (*Ly6g*$^{+/+}$)) were treated and analyzed in the same way. Each circle represents the percentage of cells carrying internalized conidia per experiment. Lines are mean ± s.d. from three independent experiments. (**f**) Production of ROS in response to phorbol myristate acetate (PMA) stimulation of isolated bone marrow neutrophils *in vitro*. Data are mean + s.d. of indicated experiments per data point and were generated in four independent experiments. MFI, mean fluorescence intensity; n.s., not significant. *P < 0.05, paired Student's t-test. (**g**) DNA NETs were induced in isolated bone marrow neutrophils using PMA stimulation. Shown are representative images of several neutrophils from wild-type or *Ly6g*$^{-/-}$ mice with the indicated polychromatic staining. Hist-H1, histone H1; MPO, myeloperoxidase. Images are representative of two independent experiments.

Neutrophils from Catchup mice function normally *in vitro*

We functionally tested neutrophils from Catchup mice under multiple conditions.

Time-lapse videomicroscopy and single-cell tracking revealed slightly but insignificantly higher velocities of neutrophils from Catchup mice compared to those from controls (**Fig. 3d** and **Supplementary Video 5**); the values correlated well with published data[24].

In phagocytosis experiments using spores of the fungus *Aspergillus fumigatus*, we detected a gradual increase in uptake over 6 h that was independent of Ly6G expression (**Fig. 3e**). The ability of Ly6G to cluster with β2-integrins (CD18) and CD11b[11] suggests a role as a coreceptor for complement receptor 3 (CD11b/CD18), allowing it to mediate the uptake of C3-opsonized *Listeria*[25]. However, uptake of opsonized and non-opsonized *Listeria* by neutrophils was indistinguishable between wild-type and homozygous Catchup mice (not shown). Furthermore, we noted unaffected abilities to produce reactive oxygen species (ROS) in response to external triggers (**Fig. 3f**) and equal neutrophil extracellular trap (NET)-formation capabilities in wild-type and Catchup neutrophils (**Fig. 3g**). Also, intracellular signaling of neutrophils in response to polyclonal external triggers was unaffected by the lack of Ly6G (**Supplementary Fig. 8**). Thus, a lack of Ly6G did not interfere with the key functions of isolated neutrophils *in vitro*.

Neutrophils from Catchup mice function normally *in vivo*

Using Catchup mice, we were able to directly test the influence of Ly6G on peritoneal recruitment without the need to use potentially function-modulating antibodies, which had yielded conflicting results before[11,12]. We compared wild-type and homozygous Catchup mice using lipopolysaccharide (LPS) peritonitis as a model[4,24]. Immigration into the LPS-inflamed peritoneum was indistinguishable between Ly6G^{-} and wild-type neutrophils (**Fig. 4a**). Thus, Ly6G was not necessary for neutrophil recruitment in this model.

Survival after lung infection with the human pathogenic fungus *A. fumigatus* is dependent on lung recruitment of neutrophils[26]. Homozygous Catchup mice were fully capable of fending off an *A. fumigatus* infection, as indicated by their weight curve

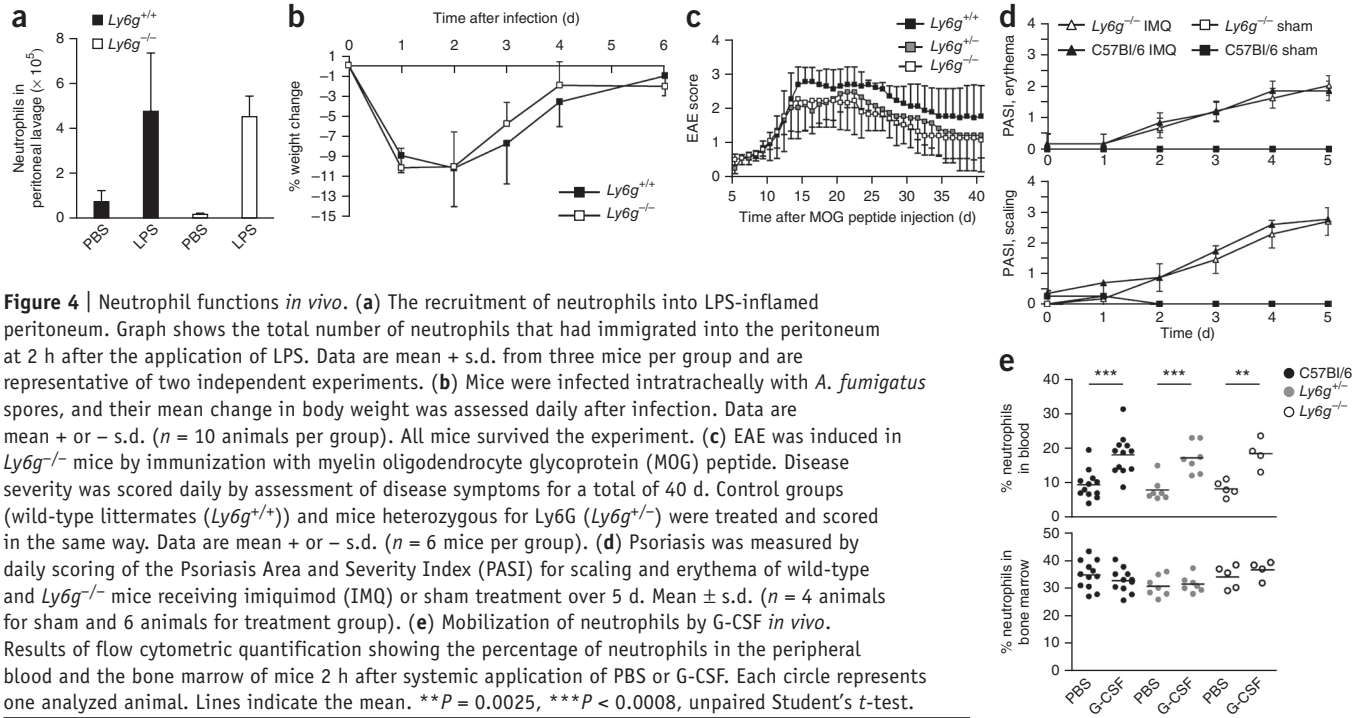

Figure 4 | Neutrophil functions *in vivo*. (**a**) The recruitment of neutrophils into LPS-inflamed peritoneum. Graph shows the total number of neutrophils that had immigrated into the peritoneum at 2 h after the application of LPS. Data are mean + s.d. from three mice per group and are representative of two independent experiments. (**b**) Mice were infected intratracheally with *A. fumigatus* spores, and their mean change in body weight was assessed daily after infection. Data are mean + or − s.d. (n = 10 animals per group). All mice survived the experiment. (**c**) EAE was induced in $Ly6g^{-/-}$ mice by immunization with myelin oligodendrocyte glycoprotein (MOG) peptide. Disease severity was scored daily by assessment of disease symptoms for a total of 40 d. Control groups (wild-type littermates ($Ly6g^{+/+}$)) and mice heterozygous for Ly6G ($Ly6g^{+/-}$) were treated and scored in the same way. Data are mean + or − s.d. (n = 6 mice per group). (**d**) Psoriasis was measured by daily scoring of the Psoriasis Area and Severity Index (PASI) for scaling and erythema of wild-type and $Ly6g^{-/-}$ mice receiving imiquimod (IMQ) or sham treatment over 5 d. Mean ± s.d. (n = 4 animals for sham and 6 animals for treatment group). (**e**) Mobilization of neutrophils by G-CSF *in vivo*. Results of flow cytometric quantification showing the percentage of neutrophils in the peripheral blood and the bone marrow of mice 2 h after systemic application of PBS or G-CSF. Each circle represents one analyzed animal. Lines indicate the mean. $^{**}P$ = 0.0025, $^{***}P$ < 0.0008, unpaired Student's t-test.

(**Fig. 4b**). Together with normal neutrophil recruitment to the lung and effective fungal clearance in $Ly6g^{+/+}$ and $Ly6g^{-/-}$ mice (**Supplementary Fig. 9**), these data indicate that Ly6G is not necessary for defense against *A. fumigatus* in neutrophils. As further evidence of a lack of function of Ly6G in fungal pathogen control, a systemic infection with *Candida albicans* was controlled in $Ly6g^{-/-}$ animals (**Supplementary Fig. 10**).

Experimental autoimmune encephalomyelitis (EAE), a model of autoimmune inflammation of the central nervous system, is promoted by early neutrophil invasion[27]. Inefficient recruitment of Ly6G$^-$ neutrophils should thus lead to less severe EAE, but heterozygous and homozygous Catchup mice behaved identically and showed insignificant differences in the progression of EAE relative to that in wild-type control animals (**Fig. 4c**). Also, the number of neutrophils recruited to the inflamed spine in Catchup mice was similar to that in wild-type mice (**Supplementary Fig. 9a**).

In a mouse model of skin irritation resembling human psoriasis, triggering the receptor TLR7 with the specific stimulus imiquimod leads to the recruitment of large numbers of neutrophils to the inflamed skin[28]. In our study, Catchup mice did not show differences in disease progression or severity (**Fig. 4d**). The cellular skin infiltrates were very similar in both genetic backgrounds (i.e., wild-type and homozygous Catchup mice), including in the number of myeloperoxidase-expressing neutrophils (not shown).

Non-inflammatory neutrophil recruitment by G-CSF is dependent on increased neutrophil motility in the bone marrow[1,2]. A single systemic pulse of G-CSF–mobilized neutrophils into the circulation in heterozygous and homozygous Catchup mice was equally effective as in controls. The relative amounts of neutrophils in the bone marrow of wild-type and Catchup mice did not change measurably during the testing period (**Fig. 4e**). We also reconstituted irradiated wild-type hosts with a 50/50 mix of bone marrow from wild-type and Catchup mice. Hematopoiesis in the hosts was equal in both types of donor bone marrow 30 and 42 d after reconstitution, as detected by equal numbers of Ly6G$^+$ and Ly6G$^-$ cells in the circulation (**Supplementary Fig. 11**). These data show the ability of $Ly6g^{-/-}$ precursors to respond normally to long-term exposure to endogenous G-CSF. Furthermore, they also demonstrated a lack of Cre-mediated cytotoxicity in neutrophils from homozygous Catchup mice, which was further confirmed by *in vitro* experiments showing equal rates of cell death in both Ly6G$^+$ and Ly6G$^-$ cells (**Supplementary Fig. 11a**).

Collectively, heterozygosity or a lack of Ly6G in Catchup mice had no detectable effect on the functionality of neutrophils *in vivo*, including on their recruitment into inflamed tissues.

FcγRIV mediates neutrophil recruitment to inflamed sites

Given the insignificance of Ly6G for neutrophil homing to inflamed sites, we wanted to study the role of FcγR in this function. FcγRIV is an activating receptor able to specifically bind IgG2a and IgG2b. It shows high expression on myeloid cells, especially monocytes and neutrophils[6], and is important for the induction of experimental epidermolysis bullosa acquisita, an autoimmune disease mediated by autoantibodies[7]. Total genetic deletion of FcγRIV prevented neutrophil recruitment into the inflamed skin and therefore inhibited disease development, but it was not possible to exclude the involvement of other myeloid cells, especially macrophages, in this phenotype[7]. Therefore, we aimed at directly testing the role of neutrophil-specific FcγRIV for recruitment into inflamed sites

Catchup mice were crossed with mice with conditional alleles of the gene encoding FcγRIV[29]. Mice with the required genetic background ($Ly6g^{+/Cre}Fcgr4^{flox/flox}$, termed CatchupR4flox) showed no abnormalities in numbers of peripheral blood monocytes or neutrophils (**Fig. 5a**). However, all peripheral blood neutrophils showed an ~55% loss of FcγRIV, whereas numbers of other FcRs on neutrophils remained unchanged. Importantly, CD11b$^+$

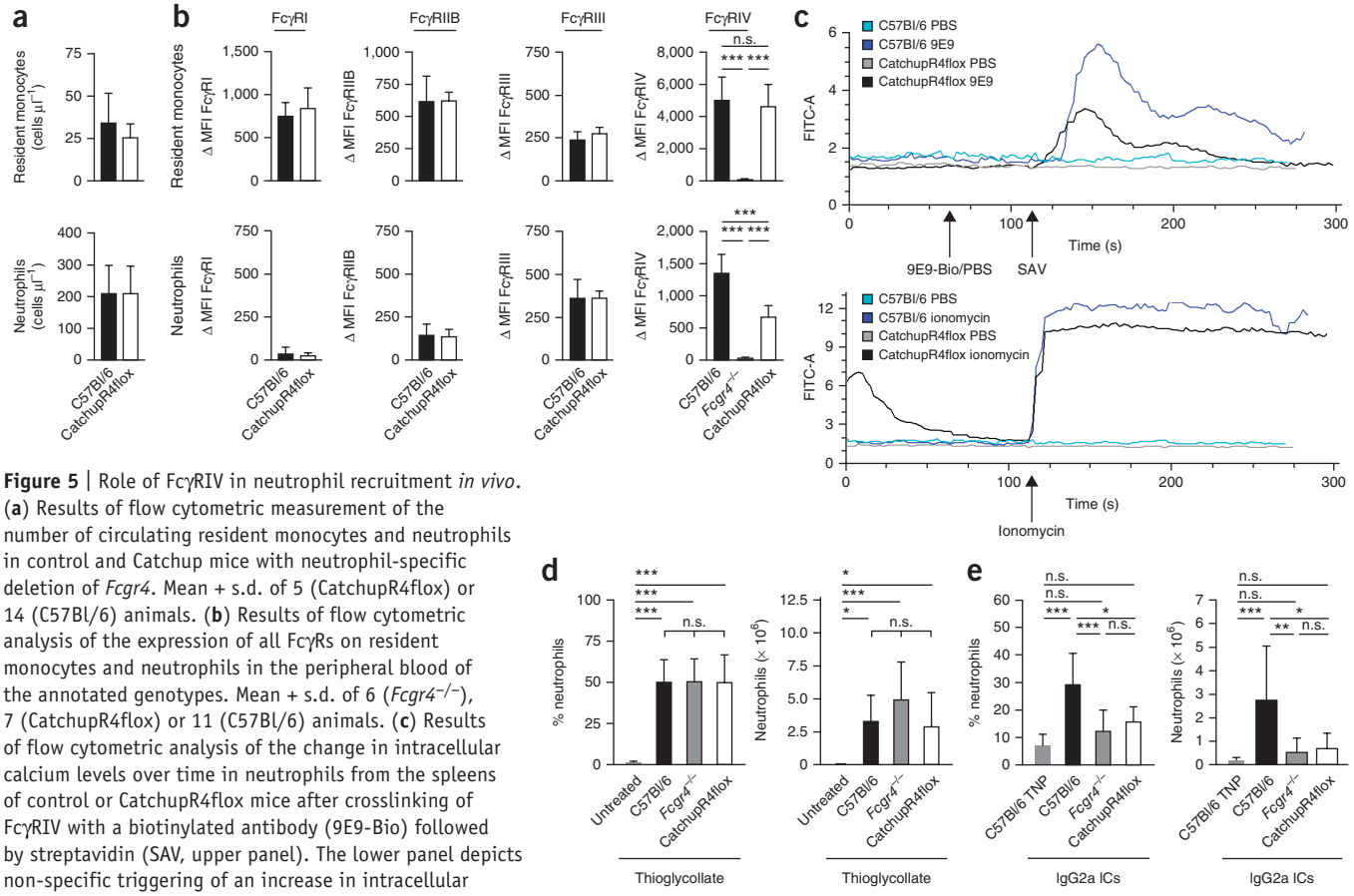

Figure 5 | Role of FcγRIV in neutrophil recruitment *in vivo*. (**a**) Results of flow cytometric measurement of the number of circulating resident monocytes and neutrophils in control and Catchup mice with neutrophil-specific deletion of *Fcgr4*. Mean + s.d. of 5 (CatchupR4flox) or 14 (C57Bl/6) animals. (**b**) Results of flow cytometric analysis of the expression of all FcγRs on resident monocytes and neutrophils in the peripheral blood of the annotated genotypes. Mean + s.d. of 6 (*Fcgr4*$^{-/-}$), 7 (CatchupR4flox) or 11 (C57Bl/6) animals. (**c**) Results of flow cytometric analysis of the change in intracellular calcium levels over time in neutrophils from the spleens of control or CatchupR4flox mice after crosslinking of FcγRIV with a biotinylated antibody (9E9-Bio) followed by streptavidin (SAV, upper panel). The lower panel depicts non-specific triggering of an increase in intracellular calcium levels using ionomycin. Data are representative of two experiments. (**d**) Analysis of the FcγRIV-independent recruitment of neutrophils of the various mouse genotypes into the peritoneum at 3 h after the injection of thioglycollate. Mean + s.d. of 7 (*Fcgr4*$^{-/-}$), 8 (CatchupR4flox), 9 (C57Bl/6) or 10 animals (untreated) analyzed in four independent experiments. (**e**) Analysis of the FcγRIV-dependent recruitment of neutrophils of the various mouse genotypes into the peritoneum at 3 h after the injection of IgG2a ICs. Mean + s.d. of 9 (*Fcgr4*$^{-/-}$), 8 (CatchupR4flox), 9 (C57Bl/6) and 7 animals (C57Bl/6 TNP) analyzed in four independent experiments. For **d** and **e** we used Student's *t*-test (2 groups) or one-way analysis of variance (≥3 groups), followed by Tukey or Bonferroni *post hoc* testing in cases of unequal variance. $*P < 0.05$, $**P < 0.01$, $***P < 0.001$.

CD62-l^{-}Gr-1^{-} resident monocytes maintained normal FcγRIV expression levels (**Fig. 5b**), demonstrating selective genetic modulation of peripheral neutrophils in Catchup mice. The deletion of the gene encoding FcγRIV by *LysM*-Cre yielded the same level of protein loss in neutrophils; however, with this Cre line, resident monocytes also lacked the gene (**Supplementary Fig. 12a**,**b**).

Neutrophils with genetically induced reductions in amounts of FcγRIV showed a strong defect in calcium flux after crosslinking of FcγRIV, a known stimulus for this FcR[6,29]. The peak height of their intracellular calcium levels was 50% lower than that in controls, whereas the general ability to flux calcium in response to ionomycin was unaffected (**Fig. 5c**). FcγRIV-dependent calcium flux was therefore directly correlated with the amount of available FcR molecules on the cell surface.

We finally asked whether the loss of FcγRIV would have an effect on neutrophil recruitment to inflamed sites *in vivo*. During thioglycollate-induced peritonitis, which is independent of FcγRIV triggering, CatchupR4flox and FcγRIV-deficient mice showed comparable recruitment of neutrophils that was similar to that in wild-type mice (**Fig. 5d**). However, peritonitis elicited by the application of IgG2a ICs induced a significant reduction of peritoneal neutrophil recruitment in CatchupR4flox mice relative to that in controls that was similar to the reduction seen in FcγRIV-deficient animals (**Fig. 5e**). Thus, the recruitment of neutrophils to areas of inflammation induced by IgG2a IC deposition is dependent on FcγRIV in a cell-autonomous manner and is not mediated by other corecruited bystander cells such as inflammatory macrophages.

DISCUSSION

Ly6G is specifically expressed by murine neutrophils. A human homolog is the GPI-anchored molecule CD177 (ref. 11). CD177, but not Ly6G, binds to PECAM-1, mediating transendothelial neutrophil migration[30]. A function in neutrophil recruitment to joint or peritoneal inflammation was reported for Ly6G (ref. 11), but this finding was challenged[12]. These studies involved the injection of Ly6G-blocking antibodies that might induce functional alterations in targeted cells[24], thereby influencing the results. Genetically induced inhibition of Ly6G expression, which we have undertaken here, is obviously a more direct approach.

Interestingly, *Ly6g* deletion in Catchup mice did not lead to phenotypic modifications in neutrophils. Functional tests, inflammatory recruitment and G-CSF mobilization were unaffected by Ly6G deficiency. Also, the reported Gr-1–mediated block in

N-formyl-methyl-leucyl-phenylalanine (fMLP)-mediated chemotaxis[11] could not be confirmed. This might have been due to the different analysis methods (videomicroscopy versus transwell migration), but more likely it was due to antibody engagement of Ly6G, which induces a signal in neutrophils that is lacking when the molecule is absent. Anti-Gr-1 is indeed able to signal in myeloid cells[31]. Homozygous Catchup mice were resistant to anti-Gr-1–mediated depletion, but some cells could still bind anti-Gr-1 to a lesser extent, possibly via Ly6C, which suggests that anti-Gr-1 binding to Ly6G depletes neutrophils, whereas its binding to Ly6C does not. Also, these data show that functional studies of Ly6G using blocking antibodies are difficult to interpret. From our findings, Ly6G also seems nonessential for neutrophil development, as we detected normal numbers of neutrophils in all measured organs of *Ly6g*$^{-/-}$ mice and effective hematopoietic reconstitution in irradiated wild-type host mice that received bone marrow from *Ly6g*$^{-/-}$ mice.

tdTomato fluorescence in Catchup mice is sufficient for flow cytometry, allowing one-step sorts of untouched, pure neutrophils from diverse tissues. Currently the most widely used mouse line for intravital neutrophil imaging is Lys-EGFP, in which neutrophils are very bright and reasonably well differentiated from other, less bright myeloid cells[32,33]. However, neutrophil depletion by a medium dose of anti-Gr-1 leaves behind a green population that is still able to invade inflamed tissues[34], making analysis of true neutrophil functions difficult. It was thus fortunate that we were able to exploit the additional Cre activity of the Catchup model using a secondary tdTomato reporter[20]. Catchup$^{IVM\text{-}red}$ mice have brightly red-fluorescent neutrophils that are well suited for intravital two-photon imaging. Use of the optimal reporter is critical, as crossing of Catchup mice to a YFP reporter[35] yielded only slightly enhanced fluorescence and low per-cell efficiency (not shown).

The exquisite neutrophil selectivity of Ly6G-driven Cre activity circumvents known problems of specificity associated with other lines, including hMRP8 (refs. 15,22). We did not observe Cre activity in immature precursors, including in GMPs, and also there was no recombination in peripheral cells from the monocyte/macrophage lineage. In contrast, hMRP8-Cre mice mainly showed monocyte-specific effects when used to study modulation of the HIF pathway *in vivo*[36]. We did see low activity in some eosinophils and basophils. Because their total number was <2% of all tdTomato^{+} cells, we do not consider them to have a major effect on neutrophil responses, and they will not confound imaging studies. Eosinophils and neutrophils in mice develop from the GMP stage[37]. Thus, tdTomato expression in some of these cells might point to prematurely terminated attempts at neutrophil development in a few precursors. Other studies used *LysM*-Cre mice to modulate genes expressed in osteoclasts[38], macrophages[39] or neutrophils[40]. As *LysM* is expressed in all these myeloid cells, the results described for these studies might be biased by the broad expression of the *LysM* promoter. In contrast to *LysM*-Cre mice, Catchup mice allow for the unequivocal investigation of neutrophil functions *in vivo*.

Our work also shows that the infiltration of neutrophils into IgG2a IC–mediated inflammation must be a cell-type-intrinsic effect mediated by FcγRIV. As the recruitment deficit was equally strong in FcγRIV-deficient mice and CatchupR4flox mice, potential migration defects in other cells might not be involved at all in the process, a discovery not possible with other systems.

We did not see a complete deletion of FcγRIV protein with this approach; in our study we noted only an ~55% reduction, although this occurred uniformly on all cells. This might be explained by the short half-life of neutrophils after the onset of Ly6G expression and point to a start of *Fcgr4* translation before neutrophil development and high stability of preformed FcγRIV protein. Quantitative PCR measurements of amounts of FcγRIV mRNA in neutrophils from CatchupR4flox mice demonstrated efficient deletion of *Fcgr4* (**Supplementary Fig. 12c**,**d**), thereby supporting such a concept. Another floxed gene was effectively deleted in Catchup-flox mice (**Supplementary Fig. 12e**), further confirming efficient genetic manipulation in this model. Protein stability will thus be the critical factor governing gene deletion in neutrophils. However, this is an intrinsic feature of the cell type, not the animal model.

METHODS

Methods and any associated references are available in the online version of the paper.

Note: Any Supplementary Information and Source Data files are available in the online version of the paper.

ACKNOWLEDGMENTS

We thank C. Kurts (University of Bonn, Germany) for helpful discussions and Imaging Center Essen (IMCES; http://imces.uk-essen.de) for help with imaging. This work was supported by the German Research Foundation (DFG; "Immunobone" to M.G. (GU769/4-1, GU769/4-2), A.W. and F.N.; SFB854 to M.G. and B.S.), the European Union (EU HEALTH-2013-INNOVATION-1, MATHIAS to M.G.) and the Mercator Research Center Ruhr (to M.G.).

AUTHOR CONTRIBUTIONS

M.G. conceived of and supervised the study and wrote the manuscript with the help of J.R.G., D.R.E. and S.B. A.H., M.H., L.M., F. Neumann, L.B., M. Stecher, A. Kraus, D.R.E., A. Klingberg, P.S., Z.A., S.K., S.E., A.R., M. Seeling, A.W., J.R.G. and F. Nimmerjahn performed experiments. S.B. provided crucial ideas. M.G., A.H., M.H., B.S. and J.R.G. discussed and interpreted results.

COMPETING FINANCIAL INTERESTS

The authors declare no competing financial interests.

1. Gunzer, M. Traps and hyper inflammation—new ways that neutrophils promote or hinder survival. *Br. J. Haematol.* **164**, 189–199 (2014).
2. Köhler, A. *et al.* G-CSF mediated thrombopoietin release triggers neutrophil motility and mobilization from bone marrow via induction of Cxcr2 ligands. *Blood* **117**, 4349–4357 (2011).
3. Sundd, P. *et al.* 'Slings' enable neutrophil rolling at high shear. *Nature* **488**, 399–403 (2012).
4. De Filippo, K. *et al.* Mast cell and macrophage chemokines CXCL1/CXCL2 control the early stage of neutrophil recruitment during tissue inflammation. *Blood* **121**, 4930–4937 (2013).
5. Lämmermann, T. *et al.* Neutrophil swarms require LTB4 and integrins at sites of cell death *in vivo*. *Nature* **498**, 371–375 (2013).
6. Nimmerjahn, F., Bruhns, P., Horiuchi, K. & Ravetch, J.V. FcgammaRIV: a novel FcR with distinct IgG subclass specificity. *Immunity* **23**, 41–51 (2005).
7. Kasperkiewicz, M. *et al.* Genetic identification and functional validation of FcgammaRIV as key molecule in autoantibody-induced tissue injury. *J. Pathol.* **228**, 8–19 (2012).
8. Jakus, Z., Nemeth, T., Verbeek, J.S. & Mocsai, A. Critical but overlapping role of FcgammaRIII and FcgammaRIV in activation of murine neutrophils by immobilized immune complexes. *J. Immunol.* **180**, 618–629 (2008).

9. Wojtasiak, M. *et al.* Depletion of Gr-1+, but not Ly6G+, immune cells exacerbates virus replication and disease in an intranasal model of herpes simplex virus type 1 infection. *J. Gen. Virol.* **91**, 2158–2166 (2010).
10. Stegemann, S. *et al.* Increased susceptibility for superinfection with *Streptococcus pneumoniae* during influenza virus infection is not caused by TLR7-mediated lymphopenia. *PLoS One* **4**, e4840 (2009).
11. Wang, J.X. *et al.* Ly6G ligation blocks recruitment of neutrophils via a beta2-integrin-dependent mechanism. *Blood* **120**, 1489–1498 (2012).
12. Yipp, B.G. & Kubes, P. Antibodies against neutrophil LY6G do not inhibit leukocyte recruitment in mice *in vivo*. *Blood* **121**, 241–242 (2013).
13. Clausen, B.E., Burkhardt, C., Reith, W., Renkawitz, R. & Forster, I. Conditional gene targeting in macrophages and granulocytes using LysMcre mice. *Transgenic Res.* **8**, 265–277 (1999).
14. Faust, N., Varas, F., Kelly, L.M., Heck, S. & Graf, T. Insertion of enhanced green fluorescent protein into the lysozyme gene creates mice with green fluorescent granulocytes and macrophages. *Blood* **96**, 719–726 (2000).
15. Passegué, E., Wagner, E.F. & Weissman, I.L. JunB deficiency leads to a myeloproliferative disorder arising from hematopoietic stem cells. *Cell* **119**, 431–443 (2004).
16. Shaner, N.C. *et al.* Improved monomeric red, orange and yellow fluorescent proteins derived from *Discosoma* sp. red fluorescent protein. *Nat. Biotechnol.* **22**, 1567–1572 (2004).
17. Becher, B. *et al.* High-dimensional analysis of the murine myeloid cell system. *Nat. Immunol.* **15**, 1181–1189 (2014).
18. Szymczak, A.L. *et al.* Correction of multi-gene deficiency *in vivo* using a single 'self-cleaving' 2A peptide-based retroviral vector. *Nat. Biotechnol.* **22**, 589–594 (2004).
19. Behnsen, J. *et al.* Environmental dimensionality controls the interaction of phagocytes with the pathogenic fungi *Aspergillus fumigatus* and *Candida albicans*. *PLoS Pathog.* **3**, e13 (2007).
20. Madisen, L. *et al.* A robust and high-throughput Cre reporting and characterization system for the whole mouse brain. *Nat. Neurosci.* **13**, 133–140 (2010).
21. Elliott, E.R. *et al.* Deletion of Syk in neutrophils prevents immune complex arthritis. *J. Immunol.* **187**, 4319–4330 (2011).
22. Abram, C.L., Roberge, G.L., Hu, Y. & Lowell, C.A. Comparative analysis of the efficiency and specificity of myeloid-Cre deleting strains using ROSA-EYFP reporter mice. *J. Immunol. Methods* **408**, 89–100 (2014).
23. King, K.Y. & Goodell, M.A. Inflammatory modulation of HSCs: viewing the HSC as a foundation for the immune response. *Nat. Rev. Immunol.* **11**, 685–692 (2011).
24. Hasenberg, M. *et al.* Rapid immunomagnetic negative enrichment of neutrophil granulocytes from murine bone marrow for functional studies *in vitro* and *in vivo*. *PLoS One* **6**, e17314 (2011).
25. Drevets, D.A. & Campbell, P.A. Roles of complement and complement receptor type 3 in phagocytosis of *Listeria monocytogenes* by inflammatory mouse peritoneal macrophages. *Infect. Immun.* **59**, 2645–2652 (1991).
26. Hasenberg, M., Stegemann-Koniszewski, S. & Gunzer, M. Cellular immune reactions in the lung. *Immunol. Rev.* **251**, 189–214 (2013).
27. Christy, A.L., Walker, M.E., Hessner, M.J. & Brown, M.A. Mast cell activation and neutrophil recruitment promotes early and robust inflammation in the meninges in EAE. *J. Autoimmun.* **42**, 50–61 (2013).
28. El Malki, K. *et al.* An alternative pathway of imiquimod-induced psoriasis-like skin inflammation in the absence of interleukin-17 receptor a signaling. *J. Invest. Dermatol.* **133**, 441–451 (2013).
29. Seeling, M. *et al.* Inflammatory monocytes and Fcgamma receptor IV on osteoclasts are critical for bone destruction during inflammatory arthritis in mice. *Proc. Natl. Acad. Sci. USA* **110**, 10729–10734 (2013).
30. Sachs, U.J. *et al.* The neutrophil-specific antigen CD177 is a counter-receptor for platelet endothelial cell adhesion molecule-1 (CD31). *J. Biol. Chem.* **282**, 23603–23612 (2007).
31. Ribechini, E., Leenen, P.J. & Lutz, M.B. Gr-1 antibody induces STAT signaling, macrophage marker expression and abrogation of myeloid-derived suppressor cell activity in BM cells. *Eur. J. Immunol.* **39**, 3538–3551 (2009).
32. Bruns, S. *et al.* Production of extracellular traps against *Aspergillus fumigatus in vitro* and in infected lung tissue is dependent on invading neutrophils and influenced by hydrophobin RodA. *PLoS Pathog.* **6**, e1000873 (2010).
33. Neumann, J. *et al.* Very-late-antigen-4 (VLA-4)-mediated brain invasion by neutrophils leads to interactions with microglia, increased ischemic injury and impaired behavior in experimental stroke. *Acta Neuropathol.* **129**, 259–277 (2015).
34. Kim, J.V., Kang, S.S., Dustin, M.L. & McGavern, D.B. Myelomonocytic cell recruitment causes fatal CNS vascular injury during acute viral meningitis. *Nature* **457**, 191–195 (2009).
35. Srinivas, S. *et al.* Cre reporter strains produced by targeted insertion of EYFP and ECFP into the ROSA26 locus. *BMC Dev. Biol.* **1**, 4 (2001).
36. Ahn, G.O. *et al.* Transcriptional activation of hypoxia-inducible factor-1 (HIF-1) in myeloid cells promotes angiogenesis through VEGF and S100A8. *Proc. Natl. Acad. Sci. USA* **111**, 2698–2703 (2014).
37. Uhm, T.G., Kim, B.S. & Chung, I.Y. Eosinophil development, regulation of eosinophil-specific genes, and role of eosinophils in the pathogenesis of asthma. *Allergy Asthma Immunol. Res.* **4**, 68–79 (2012).
38. Yang, W. *et al.* Ptpn11 deletion in a novel progenitor causes metachondromatosis by inducing hedgehog signalling. *Nature* **499**, 491–495 (2013).
39. Kleiman, A. *et al.* Glucocorticoid receptor dimerization is required for survival in septic shock via suppression of interleukin-1 in macrophages. *FASEB J.* **26**, 722–729 (2012).
40. Thompson, A.A. *et al.* Hypoxia-inducible factor 2α regulates key neutrophil functions in humans, mice, and zebrafish. *Blood* **123**, 366–376 (2014).

ONLINE METHODS

Mice. All animal experiments were conducted in accordance with German guidelines and were approved by the relevant local authorities in Essen, Mainz, Magdeburg and Erlangen. For the experiments, mice of both sexes were used, although the majority of experiments were done with female mice. Mice used were between 7 and 12 weeks old unless stated otherwise.

For the generation of Catchup mice (C57BL/6-*Ly6g*(tm2621(Cre-tdTomato)Arte)), the *Ly6g* coding sequence in exon 1 and the splice donor site at the junction of exon 1 and intron 1 were replaced with a cassette containing the open reading frame of Cre recombinase and tdTomato[16] separated by a self-splicing T2A peptide[18], thereby using the endogenous translation-initiation codon from *Ly6g* for the Cre-T2A-tdTomato construct. A polyadenylation signal (hGHpA (human growth hormone polyadenylation signal)) was inserted at the 3′ end of the Cre-T2A-tdTomato sequence in order to prevent downstream transcription of the remaining mouse *Ly6g*. The mouse genomic sequence downstream of intron 1 was left intact in order to preserve all potential regulatory elements driving the expression of *Ly6g*. The positive selection marker (puromycin resistance (PuroR)) was flanked by *FRT* sites to allow for removal after the successful generation of transgenic mice. The targeting vector was generated using BAC clones from the C57BL/6J RPCIB-731 BAC library and electroporated into TaconicArtemis C57BL/6NTac ES cell line Art B6/3.6. Positive clones were verified by PCR and Southern blot before being injected into blastocysts from superovulated BALB/c mice. Blastocysts were injected into pseudopregnant NMRI females, and the chimerism of offspring was evaluated by coat color. Highly chimeric mice were bred with C57BL/6 females mutant for the gene encoding Flp recombinase (C57BL/6-Tg(CAG-Flpe)2 Arte). Germline transmission was identified by the presence of black C57BL/6 offspring (G1). The gene encoding Flp was removed by further breeding to Flp^- partners after successful verification of PuroR removal.

Mouse genotyping. Ear biopsies of mice 6–8 weeks old were incubated at 55 °C for 3–4 h in lysis buffer containing 0.2 M NaCl, 0.1 M Tris-HCl, pH 8.5, 5 µM EDTA, 0.2% SDS and 100 µg/ml (39 U/mg) proteinase K (Sigma). After a centrifugation step, two volumes of isopropyl alcohol were added to the supernatant to precipitate genomic DNA (gDNA). 100 µl H_2O (DNase free) was added to the pellet, and subsequently gDNA was dissolved overnight at 37 °C. A maximum of 500 ng gDNA isolated from ear biopsies was used for genotyping. The typical PCR sample consisted of a 25-µl volume containing 5 pmol of the primers for PCR 1 (5065_63_for 5′-GGTTTTATCTGTGCAGCCC-3′; 5064_61_rev 5′-GAGGTCCAAGAGACTTTCTGG-3′) or for PCR 2 (2240_31_for 5′-ACGTCCAGACACAGCATAGG-3′; 5064_61_rev 5′-GAGGTCCAAGAGACTTTCTGG-3′). In both PCRs we also included a control pair of primers for amplifying CD79b as a wild-type allele (1260_for 5′-GAGACTCTGGCTACTCATCC-3′; 1260_rev 5′-CCTTCAGCAAGAGCTGGGGAC-3′). Each reaction also contained 1× Taq DNA polymerase Ready to Load Mastermix (BioBudget) with dNTPs, buffer and $MgCl_2$. The following PCR conditions were applied: 5 min, 95 °C initial denaturation; 30 s, 95 °C cyclic denaturation; 30 s, 60 °C cyclic annealing; 1 min, 72 °C cyclic elongation for a total of 35 cycles, followed by a 10-min 72 °C elongation step. All PCR protocols were developed by TaconicArtemis. PCR amplification products were analyzed by agarose gel electrophoresis.

Neutrophil depletion. In order to evaluate the neutrophil-depletion efficiency, we injected animals intraperitoneally with 100 µl anti-Gr-1 solution (clone RB6-8C5 (BioXCell) at a concentration of 1 mg/ml). 17 h later, the animals were bled by retrobulbar puncture and immediately killed by cervical dislocation. Subsequently bone marrow was flushed out of the femur and tibia of the right hind limb and resuspended in 5 ml PBS. After erythrocyte lysis (NH_4Cl (155 mM), $KHCO_3$ (10 mM), EDTA (0.1 mM)) in both cell preparations, 1×10^7 cells were stained using 70 µl of the following antibody cocktail: anti-CD45-PE-Cy7 at a final concentration of 4 µg/ml (catalog no. 552848, BD Biosciences), anti-CD11b-allophycocyanin (APC) at a final concentration of 4 µg/ml (catalog no. 101212, BioLegend) and anti-Gr-1-V450 Horizon at a final concentration of 4 µg/ml (catalog no. 560454, BD Biosciences). The percentage of neutrophils in all samples was determined by flow cytometry on a MACSQuant VYB (Miltenyi Biotec). Details about the gating strategy are explained in **Supplementary Figure 3**.

Phenotypic analysis of organs by flow cytometry. For the analysis of immune-cell ratios in organs, female animals (C57Bl/6 and $Ly6g^{-/-}$) 9–12 weeks old were killed, and the relevant organs were dissected (thymus, spleen, both inguinal lymph nodes, and bone marrow of one femur). All organs were ground through a 100-µm nylon mesh and subjected to erythrocyte lysis (NH_4Cl (155 mM), $KHCO_3$ (10 mM), EDTA (0.1 mM)). Finally, 1×10^7 cells were stained using 100 µl of different antibody solutions. Every solution contained anti-CD45-PE-Cy7 (0.4 µg/ml, catalog no. 552848, BD Biosciences). Additional antibodies used were anti-Gr1-V450 Horizon (0.2 µg/ml, catalog no. 560454, BD Biosciences) and anti-Ly6G-FITC (1 µg/ml, BD Biosciences) (cocktail a); (b) anti-F4/80-FITC (0.4 µg/ml, catalog no. ab60343, Abcam), anti-CD11b-APC (4 µg/ml, catalog no. 101212, BioLegend), and anti-Gr-1-V450 Horizon (0.2 µg/ml) (cocktail b). Both cocktails additionally contained anti-CD45. The percentage of individual cell types was determined by flow cytometry on a MACSQuant VYB (Miltenyi Biotec).

For blood-cell quantification, 500 µl blood per animal was drawn from 9-week-old female $Ly6g^{+/+}$ (C57Bl/6) or $Ly6g^{-/-}$ mice (three individuals per group) by retro-orbital puncture, placed into 1.3-ml EDTA microtubes (catalog no. 41.1504.005, Sarstedt) and kept on ice. 10 µl were subsequently probed with a veterinary hematology analyzer (Vet abc, scil) to assess blood-cell counts.

Single-cell suspensions from bone marrow and spleen were prepared as previously described[41]. Whole-blood erythrocyte lysis was carried out with hypotonic ammonium chloride solution. Prior to fluorochrome-conjugated antibody staining, Fc receptors were blocked by incubation with 2.4G2 (Becton Dickinson), except where Fc-receptor staining was required to identify GMPs. Cells were washed and incubated with different mixtures of antibodies to the following antigens: Ly6G (1A8, BD Biosciences), CD3e (145-2C11, eBioscience), CD115 (AFS98, eBioscience), B220 (RA3-6B3, eBioscience), CD11b (M1/70, BD Biosciences), CD16/32 (2.4G2, BD Biosciences), CD150 (TC15-12F12.2, eBioscience), CD41 (eBioMWReg30, eBioscience), c-Kit (ACK2, eBioscience), CD105 (MJ7/18, eBioscience), Sca-1 (D7, BD Biosciences), Nk1.1 (PK136, eBioscience), CD19 (1D3,

BD Biosciences), Ter119 (TER119, BD Biosciences), Ly6C (AL-21, BD Biosciences), Gr-1 (RB6-8C5, BD Biosciences), CD4 (RM4-5, eBioscience), CD8a (53-6.7, BD Biosciences) and TCRβ (H57-597, eBioscience). Dead cells were stained with TO-PRO-3 iodide (TOPRO) or propidium iodide (PI) as indicated in **Figure 2**. Stained cells were analyzed on an LSRFortessa flow cytometer (Becton Dickinson). Data were analyzed with FlowJo software (TreeStar). Dead cells were excluded from the analysis on the basis of TOPRO or PI and FSC/SSC gating. Cell doublets were excluded from the analysis by gating for FSC width (FSC-W) versus FSC area (FSC-A). The lineage cocktail (lin) used to exclude mature hematopoietic cells from stem and progenitor analysis contained antibodies to the following antigens (clones as mentioned above): CD3, CD4, CD8, TCRβ, CD19, B220, Nk1.1, CD11b, Gr-1 and Ter119.

Analysis of cell migration. Immediately after cervical dislocation, both hind limbs of C57Bl/6 and *Ly6g*$^{-/-}$ mice were dissected, and the bone marrow was flushed out of both the tibia and the femur by use of a 21-gauge needle attached to a 2-ml syringe filled with PBS. After centrifugation (350*g* for 5 min at room temperature) the supernatant was removed and erythrocytes were eliminated by a 10-min incubation step in 5 ml erythrocyte lysis buffer. Subsequently the remaining cells were washed once with 10 ml PBS, and neutrophils were enriched using a negative magnetic isolation kit (Miltenyi Biotec) according to the supplier's protocol and as described before[24]. Freshly isolated neutrophils were diluted to a concentration of 3.3×10^6 cells/ml in cell culture medium, and 90 µl of this suspension was placed into three channels (30 µl per channel) of a µ-Slide VI 0.4 microscopy chamber (Ibidi). The cells were incubated for 15 min at 37 °C and 5% CO_2 to let the cells attach to channel surfaces. Afterward the medium was flushed out and replaced by medium with 0.5% PBS, medium with fMLP (100 nM) or conditioned medium (CM) with PMA (10 µM). Time-lapse microscopy was conducted on a widefield microscope system (DMI 6000, Leica) at 400× magnification and 37 °C in 5% CO_2 for a duration of 4 h (three pictures per minute). The videos were subsequently analyzed using the ImageJ plugin "Manual Tracking". 15 cells per video were tracked, and the data obtained were analyzed using Chemotaxis and Migration software (Ibidi).

Analysis of cell death. Freshly isolated mouse bone marrow neutrophils were washed with PBS and subsequently resuspended in CM at a concentration of 5×10^6 cells/ml. For each time point, a separate 96-well plate was prepared with 200 µl of cell suspension containing 1×10^6 cells. Cells were incubated for 0, 2, 4, 6, 12, 24, 36 or 48 h at 37 °C and 5% CO_2. After incubation, cells were centrifuged and resuspended in 200 µl medium containing anti-Ly6G (clone 1A8, V450 Horizon, BD Bioscience), annexin V (FITC, BioLegend) and PI (0.5 mg/ml, BioLegend) in Annexin V Binding Buffer (BioLegend). The suspension was mixed and incubated for 10 min at room temperature in the dark, after which the probe was analyzed by flow cytometry.

Analysis of phagocytosis. An *A. fumigatus* spore suspension was prepared at a concentration of 1×10^8 conidia per milliliter of tap water. 1 ml of this suspension was centrifuged at 5,000*g* at room temperature for 5 min. The pellet was resuspended in 750 µl $NaHCO_3$ (0.1 M) and shaken for 30 s. The centrifugation-and-resuspension step was repeated one more time before 75 µl of pHrodo Red, SE (Life Technologies) stock solution (10 mM in dimethylsulfoxide) were added directly to the spore suspension to reach a final dye concentration of 1 mM. The staining was then conducted at room temperature in the dark for 45 min. Subsequently the spores were washed with 750 µl of washing buffer (Life Technologies) and fixed by resuspension in 1 ml 100% methanol. Immediately after the first fixation step, another 0.5 ml methanol (100%) was added, and the suspension was centrifuged in preparation for two more washing steps, each with 750 µl washing buffer. Finally the supernatant was removed and the conidia were resuspended in 1 ml PBS. Freshly isolated neutrophils were co-incubated with pHrodo-stained *A. fumigatus* conidia at a 1:5 (neutrophil:conidia) ratio at 37 °C and 5% CO_2. Control groups were treated with cytochalasin D (1 µg/ml) in parallel to inhibit phagocytosis. Subsequently the immune cells were stained with the neutrophil-specific antibody anti-Ly6G (clone 1A8) V450 Horizon (BD Biosciences), and phagocytic uptake was analyzed using a flow cytometer (MACSQuant VYB).

Analysis of ROS production. 1×10^6 neutrophils were resuspended in 1 ml cell-culture medium and stimulated with 500 nM PMA (Sigma-Aldrich) or with H_2O as a control at 37 °C for 15 min. Then the cells were immediately cooled to 4 °C, washed once with 1 ml PBS and resuspended in 500 µl ROS-detection solution (CM-H2DCFDA, Invitrogen; 1 µM in MACS buffer) together with an antibody to 1A8-Horizon V450 to simultaneously stain for Ly6G-positive events. After 20 min of incubation at room temperature, the cells were washed with 1 ml PBS, and after centrifugation (300*g* for 5 min at room temperature) the sedimented cells were dispersed in 200 µl MACS buffer and analyzed by flow cytometry for double-positive events.

Analysis of NET production. To induce the release of NET DNA, we isolated 2×10^5 neutrophils from bone marrow using a negative isolation kit (Miltenyi Biotec) and seeded them on 12-mm glass coverslips in 24-well plates. PMA was added at 100 nM to induce neutrophil activation. After incubation at 37 °C for 18 h, the cells were fixed with 2% paraformaldehyde for 20 min, blocked for 15 min using 1% BSA, and stained. Gr-1 was labeled with a primary APC-coupled antibody (BD Biosciences, 1/50). The H1 histones were primary-labeled with anti-histone H1 (Acris, BM465; 1/100) and secondary-labeled with Alexa Fluor 532–coupled goat anti-mouse IgG (Life Technologies, A11002, 1/500). To mark myeloperoxidase, we used mouse anti-human myeloperoxidase (DAKO, A0398, 1/500) coupled with Alexa Fluor 647 goat anti-rabbit (Life Technologies, A21245; 1/500). All antibodies were incubated at 37 °C for 1 h in the dark. We used 4,6-diamidino-2-phenylindole (DAPI) in ProLong Gold antifade mounting medium (Life Technologies, P36931) to stain DNA. Alternatively, Sytox Green (5 mM) was diluted 1/3,000 and incubated with the sample at room temperature for 20 min in the dark before the slides were mounted with Fluoromount G (SouthernBiotech, 0100-01) mounting medium.

Peritonitis models. LPS peritonitis was induced by i.p. injection of 15 ng LPS (Sigma-Aldrich) in 100 µl PBS or of PBS only as a control. After 2 h the peritoneum was flushed with 5 ml PBS + 5 mM EDTA. After erythrocyte lysis, neutrophils from C57Bl/6 mice were stained with an FITC-labeled Ly6G antibody (clone 1A8, BD Biosciences) and a V450-labeled Gr-1 antibody (clone

doi:10.1038/nmeth.3322

RB6-8C5, BD Biosciences) and analyzed for double-positive events. Ly6G$^-$ neutrophils were analyzed for neutrophil-specific tdTomato fluorescence. Macrophages were analyzed using an FITC-labeled F4/80 antibody (clone BM8). Immune complexes were freshly prepared by incubation of 100 µg IgG2a with 200 µg TNP-12-BSA (Biosearch) at room temperature for 3 h. Three hours after i.p. injection of 3 ml sterile 4% Brewer thioglycollate solution (w/v in H_2O, Sigma), 100 µg ICs (based on the concentration of IgG) or the respective control volume of TNP-12-BSA, the peritoneum was flushed with 10 ml PBS. After filtration and erythrocyte lysis, cells were stained with an antibody mixture containing DAPI, APC-Cy7-labeled CD45, PerCp-Cy5.5-labeled CD11b, FITC-labeled F4/80 and PE-labeled Ly6G. Data acquisition and analysis were performed using FACS Diva software (BD Biosciences). Neutrophils were gated as live CD45$^+$CD11b$^+$F4/80$^-$SSC^{hi}Ly6G$^+$ cells after the exclusion of doublets.

***A. fumigatus* infection.** We induced a pulmonary mold infection by intratracheally applying 5×10^6 resting *A. fumigatus* spores (strain ATCC 46645) suspended in 100 µl sterile tap water. For this, male or female mice 10–12 weeks old were anesthetized by an i.p. injection of ketamine/xylazine at a final concentration of 60/6 mg/kg. After reaching deep narcosis, the animals were intubated using a 22-gauge indwelling venous catheter (Vasofix Braunüle, B. Braun AG), and the spore suspension was applied. To achieve a better distribution of the spore mass and to avoid suffocation, we ventilated the animals for 1 min with a small-animal respirator (MiniVent, Hugo Sachs) at a rate of 250 breaths per minute and an inhalation volume of 300 µl per breath. During the next 4 d we monitored the body weight and general health status of all animals. The C57Bl/6 group and the *Ly6g*$^{+/-}$ group contained five individuals each, and the *Ly6g*$^{-/-}$ group was composed of ten animals. For quantification of infiltrated neutrophils, lungs were flushed with PBS, stained for CD45 and Ly6G and analyzed by flow cytometry. For measurement of colony-forming units (CFU), 8-week-old *Ly6g*$^{-/-}$ mice, or C57/BL6 mice as controls, were infected intratracheally with *A. fumigatus* (5×10^6 conidia), and lungs were harvested into C-tubes (Miltenyi Biotec) with 2 ml PBS at the time points indicated in **Supplementary Figure 9b**,**c**. The lungs were then dissociated with the GentleMACS Dissociator (Miltenyi Biotec), running lung programs 1 and 2, and 100 µl of lung suspension were plated in different dilution steps on *Aspergillus* minimal medium. CFU were read out after 24 h of incubation at 37 °C.

***C. albicans* infection.** *C. albicans* was grown overnight at 30 °C in yeast-peptone-glucose (YPG) broth. Cultures were diluted 1:50 and grown again in fresh YPG medium. Cells were harvested at the logarithmic growth phase (OD_{600} = 0.5–1.0) and were washed three times with PBS. Mice were infected with 1×10^5 CFU intravenously.

Experimental autoimmune encephalomyelitis. Active EAE was induced by injection of 200 µg MOGp35-55-peptide emulsified in 200 µl complete Freund's adjuvant containing 800 µg heat-killed *Mycobacterium tuberculosis*. A volume of 50 µl was injected subcutaneously into the flanks at four sites. Additionally, 200 ng pertussis toxin dissolved in 200 µl PBS was injected intraperitoneally on day 0 and 2 d after immunization. The clinical signs of EAE were monitored daily and scaled as follows: 0, no signs of disease; 0.5, partial loss of tail tonus; 1, limp tail; 1.5, limp tail and slight slowing of righting; 2, partial paresis of one hind limb; 2.5, dragging of hind limbs without total paresis; 3, complete paralysis of at least one hind limb; 4, severe forelimb weakness; 5, moribund or dead. The daily clinical score of each group was calculated as the average of all individual disease scores. Animal experiments were approved by the local state authorities. Mice with clinical scores above 3 were killed according to the relevant animal statutes.

Psoriasis. Female mice at the age of 7–8 weeks were treated with Aldara (5% imiquimod; Meda AB) or Sham cream[42] on ears (each with 5 mg) and the skin of the back (50 mg) for five consecutive days. To measure the severity of inflammation on the back, we used a scoring system similar to the human PASI. To calculate this score in mice, we considered the parameters of skin thickness, scaling and erythema. The individual scores for scaling and erythema are shown in **Figure 4d**.

G-CSF mobilization. Mice were injected intravenously with 25 µg/ml hG-CSF (Neupogen Amgen GmbH) in a volume of 100 µl PBS or with PBS only as a control as described[2]. After 2 h, 75 µl peripheral blood was collected by retro-orbital puncture. After erythrocyte lysis, cells from C57Bl/6 and *Ly6g*$^{+/-}$ mice were stained with an FITC-stained Ly6G antibody (clone 1A8, BD Biosciences) and a V450 Horizon–stained Gr-1 antibody (clone RB6-8C5, BD Biosciences) and analyzed for double-positive events using a MACSQuant VYB flow cytometer (Miltenyi Biotec). Cells from *Ly6g*$^{-/-}$ mice were analyzed for neutrophil-specific tdTomato fluorescence.

Generation of mixed bone marrow chimeras. Bone marrow cells from Ly6G-competent (CD45.2$^+$Ly6G$^+$) and Ly6G-deficient (CD45.2$^+$Ly6G$^-$) mice were mixed at a 1:1 ratio, and a total of 5×10^6 cells was injected intravenously into lethally irradiated (9 Gy) congenic CD45.1$^+$ mice.

Intravital two-photon microscopy. Mice were prepared for intravital microscopy of long bones as previously described[2]. Two-photon microscopy of the tibia was performed using a Leica TCS SP8 MP microscope with simultaneous detection via hybrid reflected-light detectors and an HCX IRAPO L 25×/0.95-NA (numerical aperture) water-immersion objective. Illumination was performed at 1,050 nm using a Coherent Chameleon Vision II Ti:sapphire laser. The tdTomato-fluorescent neutrophils were detected with a 585/50 filter, and bone was detected by its second-harmonic-generation (SHG) signal with a 525/50 filter. Blood vessels were visualized by i.v. injection of Q-Dots (QTracker 655, Life Technologies; 1 µM in 100 µl PBS). Videos were recorded over 30 time points (1 time point ≈ 1 min). The raw data were reconstructed using Imaris software (Bitplane) and connected to the final videos using PowerPoint (Microsoft) for shift removal and ImageJ (US National Institutes of Health) for labeling and combining.

Identification of cellular subtypes. For the identification of eosinophils and basophils, cells from erylysed blood were stained with anti-Siglec-F (clone E50-2440, BD Biosciences), anti-CD11c (clone N418, BioLegend), anti-CD45 (clone Ly-5, BD Biosciences), anti-FcεRI (clone MAR-1, BioLegend) or anti-CD49b (clone HMα2, BioLegend). Analysis was performed on a MACSQuant

VYB (Miltenyi Biotec) after gating on single cells. For identification of microglia and Kupffer cells by *ex vivo* brain and liver imaging, Catchup$^{IVM\text{-}red}$ and CX3CR1-GFP mice were used. Mice received 10 µg CD31-PE (BD Biosciences, catalog no. 553373) intravenously and were killed 20 min after injection. The liver and brain were directly removed and transferred to PBS warmed to 37 °C. For *ex vivo* two-photon imaging of the brain and liver, sequential scans were used. For excitation of Ly6G, the two-photon laser was tuned to 1,050 nm, and therefore the SHG signal was generated at 525 nm. As a second sequence for the excitation of GFP and CD31-PE, the laser was tuned to 960 nm. Ly6G and GFP were detected via hybrid detectors, and SHG and CD31-PE signals were detected via photomultipliers. All data were visualized via Imaris. For analysis of the cells by flow cytometry, mice were perfused via the portal vein with a 0.05% collagenase solution. Organs were cut into small pieces and digested for 20 min at 37 °C in Gey's balanced salt solution with 0.04% collagenase, and the resulting material was then filtered through a 250-µm cell strainer. Cells were resuspended in PBS and subjected to flow cytometry. For the isolation of Kupffer cells, digested liver homogenates were centrifuged (25% and 50% Percoll-gradient centrifugation) for 30 min at 1,350*g* at 4 °C. After centrifugation, cells from the interface were collected and subjected to flow cytometry.

Sorting and cytospins. Whole bone marrow cells from both femurs of C57Bl/6, Catchup or Catchup$^{IVM\text{-}red}$ mice (males and females, 12–31 weeks old) were flushed out using 10 ml PBS + 10% fetal calf serum (FCS) and stored on ice. Right before they were sorted, the cells were spun down (400*g* for 5 min at room temperature), resuspended in 10 ml MACS buffer (PBS + 2 mM EDTA + 1% FCS) and filtered through a 70-µm cell strainer. Using a 70-µm nozzle and the sorting mode "Purity," cells were separated on a FACS ARIA III (BD Biosciences) according to the templates shown in **Supplementary Figure 7a**. For evaluation of cell morphology, 2×10^5 cells of all relevant subpopulations before and after sorting were spun onto glass slides using a cytocentrifuge (Shandon Cytospin 2, Shandon Southern Instruments) and Wright stained. Parallel samples of all populations (1×10^5 cells in 150 µl PBS + 10% FCS) were transferred into Press-to-Seal silicon chambers (Life Technologies; 20-mm diameter, 0.5-mm height) and analyzed for their tdTomato-fluorescence intensity on a Leica DMI6000 widefield microscope system (excitation filter, 555 ± 12.5; emission filter, 605 ± 26). Optimal camera and illumination settings for slight fluorescence saturation were identified for Tomato^{hi} neutrophils from Catchup$^{IVM\text{-}red}$ mice, and these parameters were kept constant for all other cells. A third fraction of all cell populations (2×10^5 cells) was analyzed by flow cytometry on a MACSQuant VYB (Miltenyi Biotec). To identify leukocytes, we stained the cells with anti-CD45 (BD Biosciences, catalog no. 552848; final concentration, 0.4 µg/ml).

Intracellular calcium measurements. Spleen cells were isolated, and erythrocytes were lysed and then washed twice in PBS. After being stained with APC-labeled antibodies against CD19 and TCRβ for 20 min at 4 °C in an overhead rotor and centrifuged, cells were resuspended in 1× PBS and loaded for 30 min at 25 °C with an equal amount of 2.5 M Fluo-3-AM (acetoxymethyl) solution (Biotium). To allow AM hydrolyzation by intracellular esterases, we incubated cells at 37 °C for 30 min in PBS after an additional PBS-washing step. Finally cells were washed twice with Krebs Ringer solution (KRS) containing 1% FCS. Two minutes before analysis, cells were prewarmed in already warm KRS–1% FCS. Neutrophils were gated as singlets, CD19$^-$TCRβ$^-$ and SSC^{hi} cells. Data acquisition was done with the following pattern: 1-min acquisition to establish the baseline of the Fluo-3-AM signal (basal intracellular calcium concentration), 1-min acquisition after the addition of 4 µg 9E9-biotin or the same volume of PBS, and 3-min acquisition after the addition of 8 µg streptavidin. For the positive control, we added 1.5 µg ionomycin (Sigma) after the baseline had been acquired for 2 min. Data acquisition was performed using FACS Diva software (BD Biosciences).

qRT-PCR. Total RNA was extracted from sorted spleen neutrophils (RNeasy Micro Kit, Qiagen), and 50 ng was transcribed into cDNA using an AffinityScript Multiple Temperature cDNA Synthesis Kit (Agilent Technologies) with the following gene-specific primers: *Actb*, 5′-TGTCCACCTTCCAGCAGATGT-3′ (forward), 5′-AGCTCAGTAACAGTCCGCCTAGA-3′ (reverse); *Fcgr4*, 5′-GGGCTCATTGGACACAACA-3′ (forward), 5′-ATG GATGGAGACCCTGGAT-3′ (reverse). To determine the expression of *Fcgr4* relative to that of the ubiquitously expressed housekeeping gene *Actb*, we used the Brilliant III Ultra Fast SYBR Green QPCR Master Mix Kit (Agilent Technologies). tdTomato$^+$ cells from *Ly6g*$^{+/-}$ and Ly6GIL1R2fl/fl mice were sorted by FACS (BD Aria III) and used for total RNA isolation using the peqGOLD Total RNA Kit (Peqlab). qRT-PCR was performed with the QuantiTect SYBR Green RT-PCR Kit using primers from Qiagen as described online (http://www.qiagen.com/products/pcr/quantitect/primerassays.aspx). All changes in gene expression were calculated relative to that of the gene encoding hypoxanthine-guanine phosphoribosyltransferase.

Signaling. Neutrophils were isolated with the neutrophil-isolation kit from Miltenyi according to the manufacturer's protocol. 6×10^6 freshly isolated neutrophils from *Ly6g*$^{+/+}$ and *Ly6g*$^{-/-}$ mice were either stimulated with PMA (100 ng/ml) for 10 and 30 min or left unstimulated. For western blot analysis, cellular extracts from 3×10^6 cells were obtained. The blots were reprobed with the antibodies indicated in **Supplementary Figure 8c**. For flow cytometry analysis, 3×10^6 cells were used for surface staining with antibodies to CD45, CD11b and Ly6G. Subsequent fixation, permeabilization and intracellular staining with pErk antibody were performed with an intracellular staining kit from eBioscience according to the manufacturer's instructions. Phosphorylation of Erk in neutrophils from *Ly6g*$^{+/+}$ and *Ly6g*$^{-/-}$ mice was determined in live CD45$^+$CD11b$^+$Ly6G$^+$ and CD45$^+$CD11b$^+$Tomato$^+$ neutrophils, respectively.

Statistics. We used GraphPad Prism to calculate statistical significance. Data were analyzed using Student's *t*-test or one-way analysis of variance, followed by Tukey or Bonferroni *post hoc* testing in cases of unequal variance. *P* values less than 0.05 were considered significant.

41. Sprüssel, A. *et al.* Lysine-specific demethylase 1 restricts hematopoietic progenitor proliferation and is essential for terminal differentiation. *Leukemia* **26**, 2039–2051 (2012).
42. Heib, V. *et al.* Mast cells are crucial for early inflammation, migration of Langerhans cells, and CTL responses following topical application of TLR7 ligand in mice. *Blood* **110**, 946–953 (2007).

doi:10.1038/nmeth.3322